Circulation

ORIGINAL RESEARCH ARTICLE

Interferon-γ Impairs Human Coronary Artery Endothelial Glucose Metabolism by Tryptophan Catabolism and Activates Fatty Acid Oxidation

Laurel Yong-Hwa Lee, MD, DPhil; William M. Oldham, MD, PhD; Huamei He, MD, PhD; Ruisheng Wang, PhD; Ryan Mulhern, BA; Diane E. Handy, PhD; Joseph Loscalzo, MD, PhD

BACKGROUND: Endothelial cells depend on glycolysis for much of their energy production. Impaired endothelial glycolysis has been associated with various vascular pathobiologies, including impaired angiogenesis and atherogenesis. IFN-γ (interferon-γ)–producing $CD4^+$ and $CD8^+$ T lymphocytes have been identified as the predominant pathological cell subsets in human atherosclerotic plaques. Although the immunologic consequences of these cells have been extensively evaluated, their IFN-γ–mediated metabolic effects on endothelial cells remain unknown. The purpose of this study was to determine the metabolic consequences of the T-lymphocyte cytokine, IFN-γ, on human coronary artery endothelial cells.

METHODS: The metabolic effects of IFN-γ on primary human coronary artery endothelial cells were assessed by unbiased transcriptomic and metabolomic analyses combined with real-time extracellular flux analyses and molecular mechanistic studies. Cellular phenotypic correlations were made by measuring altered endothelial intracellular cGMP content, wound-healing capacity, and adhesion molecule expression.

RESULTS: IFN-γ exposure inhibited basal glycolysis of quiescent primary human coronary artery endothelial cells by 20% through the global transcriptional suppression of glycolytic enzymes resulting from decreased basal HIF1α (hypoxia-inducible factor 1α) nuclear availability in normoxia. The decrease in HIF1α activity was a consequence of IFN-γ–induced tryptophan catabolism resulting in ARNT (aryl hydrocarbon receptor nuclear translocator)/HIF1β sequestration by the kynurenine-activated AHR (aryl hydrocarbon receptor). In addition, IFN-γ resulted in a 23% depletion of intracellular nicotinamide adenine dinucleotide in human coronary artery endothelial cells. This altered glucose metabolism was met with concomitant activation of fatty acid oxidation, which augmented its contribution to intracellular ATP balance by >20%. These metabolic derangements were associated with adverse endothelial phenotypic changes, including decreased basal intracellular cGMP, impaired endothelial migration, and a switch to a proinflammatory state.

CONCLUSIONS: IFN-γ impairs endothelial glucose metabolism by altered tryptophan catabolism destabilizing HIF1, depletes nicotinamide adenine dinucleotide, and results in a metabolic shift toward increased fatty acid oxidation. This work suggests a novel mechanistic basis for pathological T lymphocyte–endothelial interactions in atherosclerosis mediated by IFN-γ, linking endothelial glucose, tryptophan, and fatty acid metabolism with the nicotinamide adenine dinucleotide balance and ATP generation and their adverse endothelial functional consequences.

Key Words: coronary artery ■ endothelium ■ fatty acid oxidation ■ glycolysis ■ interferon-γ ■ metabolism ■ tryptophan

Correspondence to: Joseph Loscalzo, MD, PhD, Department of Medicine, Brigham and Women's Hospital and Harvard Medical School, 75 Francis St, Boston, MA 02115. Email jloscalzo@rics.bwh.harvard.edu

Supplemental Material is available with this article at https://www.ahajournals.org/doi/suppl/10.1161/CIRCULATIONAHA.121.053960.

For Sources of Funding and Disclosures, see page 1626.

Circulation is available at www.ahajournals.org/journal/circ

Clinical Perspective

What Is New?

- IFN-γ (interferon-γ), a major cytokine in human atheroma secreted by $CD8^+$ and $CD4^+$ T lymphocytes, impairs glucose metabolism of primary human coronary artery endothelial cells by inhibiting glycolysis and depleting nicotinamide adenine dinucleotide (NAD[H]).
- Glycolysis inhibition by IFN-γ was mediated by hypoxia-inducible factor 1α destabilization resulting from tryptophan catabolism to kynurenine with downstream sequestration of hypoxia-inducible factor 1β by the aryl hydrocarbon receptor and was offset by increased fatty acid oxidation to preserve cellular energy balance.
- IFN-γ–induced metabolic derangements were accompanied by adverse endothelial phenotypic changes, including intracellular cGMP depletion, impaired migratory capacity, and increased adhesion molecule expression.

What Are the Clinical Implications?

- Endothelial cells depend on glycolysis for energy, angiogenesis, and survival, and their impairment by IFN-γ in atheroma-laden coronary artery endothelium likely accelerates atherosclerosis and impairs collateral vessel formation.
- Our metabolomic and transcriptomic analyses demonstrate that IFN-γ induces widespread perturbations across a network of metabolic pathways (glycolysis, NAD[H], tryptophan, and fatty acid metabolism) and regulatory and signaling pathways (hypoxia-inducible factor 1, AMP-activated protein kinase, NO-cGMP) essential for vascular homeostasis and function, highlighting the fluid crosstalk between, and cross-regulation of, multiple endothelial metabolic pathways in coronary artery disease.
- This study provides a novel pathobiological mechanism linking T cell activation and coronary artery disease through endothelial metabolic derangements by IFN-γ.

Nonstandard Abbreviations and Acronyms

ADP	adenosine diphosphate
AHR	aryl hydrocarbon receptor
ARNT	aryl hydrocarbon receptor nuclear translocator
ATP	adenosine triphosphate
CPT1	carnitine palmitoyl transferase I
FAO	fatty acid oxidation
HCAEC	human coronary artery endothelial cell
HIF1	hypoxia-inducible factor 1
IDO1	indoleamine 2,3,-dioxygenase 1
IFN-γ	interferon-γ
LDHA	lactate dehydrogenase A
NAD	nicotinamide adenine dinucleotide
OCR	oxygen consumption rate
PARP	poly (ADP-ribose) polymerase

Glucose metabolism is fundamental to endothelial cell survival and function, serving as an essential source for energy generation, biomass synthesis, and redox hemostasis (see review[1]). Endothelial cells depend on glycolysis for much of their ATP (adenosine triphosphate) production, up to 80% even in the presence of abundant oxygen,[2,3] and on the pentose phosphate pathway for redox balance and nucleotide synthesis. Dysregulated endothelial glycolysis has been linked to various vascular pathologies, including atherogenesis,[4] pulmonary hypertension,[5] and impaired angiogenesis.[6]

The interface between the immunologic and endothelial systems forms a shared mechanistic basis for a broad spectrum of diseases, including atherosclerosis. IFN-γ (interferon-γ)–producing $CD8^+$ and $CD4^+$ T helper type 1 cells have been identified as the most abundant and prominent pathological immune cell subsets in human carotid atherosclerotic plaques correlating with worse clinical outcomes.[7] IFN-γ has been characterized as proatherogenic in mice[8,9] and has been linked to neointima formation in in-stent stenosis[10] and allograft vasculopathy[11] in humans. Although their contributions as immune effector cells to atheroma development and progression have been extensively studied, the metabolic consequences of their actions, and of IFN-γ in particular, on endothelial cells remain unknown.

Here we study the metabolic effects of IFN-γ on human coronary artery endothelial cells (HCAECs) with unbiased transcriptomic and metabolomic analyses. Given that most systemic vascular beds affected by atherosclerosis are nonproliferating in the absence of significant hypoxic stress, our study focuses on how basal metabolism of quiescent endothelial cells is altered by IFN-γ exposure in normoxia. We demonstrate that IFN-γ exposure results in significant impairment of basal endothelial glucose metabolism by altered tryptophan metabolism with downstream inhibition of HIF1 (hypoxia-inducible factor 1) activity resulting from AHR (aryl hydrocarbon receptor) activation by the tryptophan catabolite kynurenine. These effects are accompanied by concomitant intracellular nicotinamide adenine dinucleotide depletion and heightened endothelial oxygen consumption from accelerated fatty acid oxidation, and are associated with endothelial dysfunction. These metabolic derangements and their associated pathological phenotypic changes present a novel mechanistic link between the endothelial cell and T cell–dependent, IFN-γ–mediated cardiovascular pathobiology.

METHODS

An expanded methods section is provided in the Supplemental Material.

Data Availability

The data that support the findings of this study are available from the corresponding author on reasonable request.

No animal experiments were included in this study. Although we used human cells, they were purchased from a vendor, Lonza. They were anonymous with respect to donor, and institutional review board review was not required.

Cell Culture and Treatments

Primary HCAECs (Lonza) were cultured in Endothelial Cell Growth Basal Medium-2 supplemented with EGM-2 Microvascular Endothelial Cell Growth Medium-2 BulletKit without antibiotics unless otherwise specified at 37°C with 5% CO_2. Glucose concentration of this medium was 1.0 g/L (5.5 mM) unless otherwise indicated. Low- and high-glucose media were prepared using the basal medium containing no glucose (Cell Biologics) with the BulletKit supplemented with glucose (Boston Bioproducts) at 2.5 mM and 25 mM, respectively. For studying the effects of tryptophan depletion, confluent HCAECs were incubated with DMEM containing 1.0 g/L glucose and deficient in tryptophan (Thermo Fisher Scientific) with or without exogenous tryptophan supplementation (16.0 mg/L; Sigma) equivalent to the concentration in the standard DMEM formulation. The cells had been prepared commercially from deceased adult male and female donors ranging in age from 46 to 55 years without diabetes or known cardiac diseases whose causes of deaths were noncardiac. All experiments were performed with cells grown to confluence between passages 5 and 7 before being treated with human recombinant IFN-γ (R&D Systems; 1–50 ng/mL) in vitro for the durations specified. For the real-time extracellular flux assays and high-performance liquid chromatography measurements of ATP and ADP (adenosine diphosphate), only passage 6 cells were used. For indoleamine 2,3,-dioxygenase 1 (IDO1) inhibition, cells were cotreated with 1-methyltryptophan (Sigma-Aldrich; 1, 3, and 5 mM) and IFN-γ at 50 ng/mL for 24 h. For poly (ADP-ribose) polymerase (PARP) inhibition, cells were pretreated with 3-aminobenzamide (Sigma-Aldrich; 5 mM) for 1 hour before 24 hours of IFN-γ treatment. For nicotinamide adenine dinucleotide (NAD) precursor supplementation, nicotinamide mononucleotide was added at 0.5 mM to cells pretreated with IFN-γ for 24 hours for an additional 24 hours before measuring total intracellular NAD (NAD[H]). For fatty acid oxidation (FAO) inhibition, 2[6(4-chlorophenoxy)hexyl]oxirane-2-carboxylate (etomoxir; Cayman; 10 μM) was added during the last hour of 24 hours of IFN-γ treatment at 50 ng/mL. For hypoxia studies, cells were treated for 24 hours with 1% O_2, 5% CO_2, with N_2 balance, at 37°C in a hypoxia chamber glove box with or without IFN-γ at 50 ng/mL.

Statistical Analyses

Statistical analyses were performed with GraphPad Prism 8. Data represent mean±SEM from at least 3 independent experiments as specified. Normal distribution was assessed by the Shapiro-Wilk test. Homogeneity of variances was assessed by the F test or Brown-Forsythe test. For normally distributed data, 2-tailed Student *t* test or Welch's *t* test (for unequal variances) was used for 2-group analyses, and 1- or 2-way ANOVA with post hoc Bonferroni, Tukey, or Sidak multiple comparisons test or Welch's ANOVA test (for unequal variances) with post hoc Dunnett T3 multiple comparisons test was used for multigroup analyses, as specified. For data that deviate from a normal distribution, the Mann-Whitney *U* test or Wilcoxon matched-pairs signed-rank test was used for 2-group analyses, and the Kruskal-Wallis test with post hoc Dunn multiple comparisons test was used for multigroup analyses. One-sample *t* test was used to analyze the fold changes in normalized protein densitometric analysis data or intracellular cGMP as specified. $P<0.05$ was used to define statistical significance.

RESULTS

IFN-γ Impairs Basal Glycolysis in HCAECs

IFN-γ exposure to confluent, resting HCAECs for 24 hours in vitro in culture medium containing physiological glucose concentration (5.5 mM) resulted in a 20% decrease in basal extracellular acidification rate ($P=0.006$) measured by the real-time extracellular flux assay, indicating decreased endothelial glycolytic activity (Figure 1A). Consistent with this finding, a 27% decrease in intracellular lactate was observed ($P=0.010$) (Figure 1B).

HCAECs exposed to IFN-γ had significantly reduced intracellular glucose transport in vitro as demonstrated by a 20% decrease in the fluorescent glucose analogue 2-(N-(7-nitrobenz-2-oxa-1,3-diazol-4-yl)amino)-2-deoxyglucose uptake (Figure 1C and 1D). Similarly, many of the intracellular intermediates in glycolytic pathways measured by liquid chromatography mass spectrometry, including fructose-1,6-bisphosphate, dihydroxyacetone phosphate, glyceraldehyde 3-phosphate, phosphoenolpyruvate, and pyruvate, were significantly decreased after 24 hours of IFN-γ exposure throughout (Figure 1E–1I). Together, these findings indicate that IFN-γ impairs endothelial glycolysis (Figure 1O). Similarly, impaired glycolysis was observed in the absence of serum or growth factor supplementation to the culture medium and, in addition, in low-glucose medium (2.5 mM) (Figure S1).

IFN-γ Induces Global Suppression of Endothelial Glycolytic Enzyme Gene Expression

Given the notable suppression of basal glycolysis, including glucose uptake and pyruvate-to-lactate conversion, we hypothesized that IFN-γ impairs glycolysis by inhibition of multiple glycolytic enzymes at the transcriptional level. Indeed, expression of both *SLC2A1* (solute carrier family 2 member 1) and *LDHA* (lactate dehydrogenase A), the genes encoding the enzymes regulating glucose uptake and pyruvate-to-lactate conversion, respectively, was suppressed after 24 hours of IFN-γ exposure in

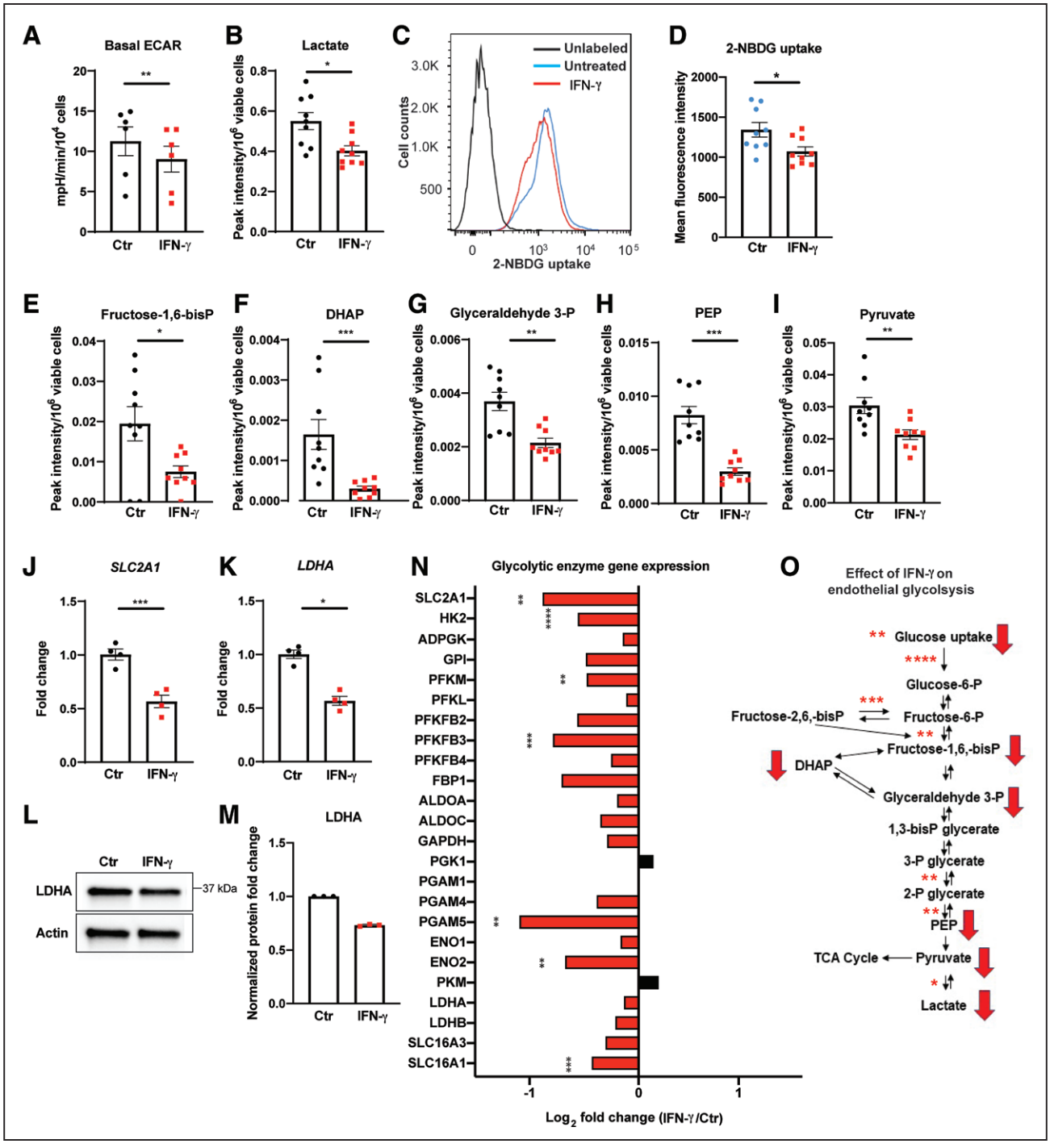

Figure 1. IFN-γ impairs basal glucose metabolism in HCAECs by global transcriptional suppression of glycolytic enzymes. **A**, Real-time extracellular flux analysis of extracellular acidification rate (ECAR) of human coronary artery endothelial cells (HCAECs) after 24 hours of IFN-γ treatment at 50 ng/mL. Data represent mean±SEM from 6 independent experiments. **B**, Intracellular lactate levels in HCAECs measured by LC-MS after the same IFN-γ treatment. Mean±SEM from 9 biological replicates from 3 independent experiments. **C** and **D**, Cellular uptake of the glucose analogue 2-NBDG by HCAECs assessed by flow cytometry after 48 hours of IFN-γ treatment. Mean±SEM from 9 biological replicates from 3 independent experiments. **E** through **I**, Intracellular metabolites of the glycolytic pathway in HCAECs measured by LC-MS after 24 hours of IFN-γ treatment. Mean±SEM from 9 biological replicates from 3 independent experiments. **J** and **K**, Gene expression changes of *SLC2A1* (**J**) and *LDHA* (**K**) measured by real-time PCR in HCAECs after the same IFN-γ treatment. Mean±SEM from 4 independent experiments. Statistical significance was assessed using paired (**A**) or unpaired (**D**) 2-tailed Student *t* tests, unpaired Welch *t* tests (**B, E, I,** and **J**), and Mann-Whitney *U* tests (**F**–**H** and **K**). **L** and **M**, Protein expression changes of LDHA by Western blot in HCAECs after 24 to 48 hours of IFN-γ (**L**) and densitometric quantification of 3 independent experiments (**M**). **N**, IFN-γ–induced gene expression changes involving the glycolytic enzymes by RNA sequencing analysis of HCAECs obtained in biological triplicates. Statistical significance was determined on the basis of the *P* values adjusted for multiple test hypotheses by the Benjamini-Hochberg procedure with a false discovery rate threshold of <0.05. (*Continued*)

Figure 1 Continued. O, Summary of IFN-γ impairment of HCAEC glycolysis at the transcriptional (asterisks) and metabolite (red arrows) levels. Red arrows denote the significantly decreased intracellular metabolites measured by LC-MS, whereas asterisks indicate the significantly decreased gene expressions of the enzymes involved in the reactions and the extents of the statistical significance. 1,3-bisP glycerate indicates 1,3-bisphosphoglycerate; 2-NBDG, 2-(N-(7-nitrobenz-2-oxa-1,3-diazol-4-yl)amino)-2-deoxyglucose; 2-P glycerate, 2-phosphoglycerate; 3-P glycerate, 3-phosphoglycerate; ADPGK, ADP-dependent glucokinase; ALDO, aldolase, Ctr, control; DHAP, dihydroxyacetone phosphate; ENO, enolase; FBP1, fructose-bisphosphatase 1; fructose-1,6-bisP, fructose-1,6,-bisphosphate; fructose-2,6-bisP, fructose-2,6,-bisphosphate; fructose-6-P, fructose-6-phosphate; GPI, glucose-6-phosphate isomerase; glucose-6-P, glucose-6-phosphate; glyceraldehyde 3-P, glyceraldehyde 3-phosphate; HK, hexokinase, IFN, interferon; LC-MS, liquid chromatography mass spectrometry; LDH, lactate dehydrogenase; PEP, phosphoenolpyruvate; PFK, phosphofructokinase; PFKFB, 6-phosphofructo-2-kinase/fructose-2,6-biphosphatase; PGAM, phosphoglycerate mutase; PGK, phosphoglycerate kinase; PKM, pyruvate kinase M; SLC16A1, solute carrier family 16A member 1 (encodes monocarboxylate transporter 1); SLC16A3, solute carrier family 16A member 3 (encodes monocarboxylate transporter 4); SLC2A1, solute carrier family 2 member 1; and TCA, tricarboxylic acid. *P<0.05; **P<0.01; ***P<0.001; ****P<0.0001.

vitro, each by >40% (P=0.0008 and 0.0286, respectively) (Figure 1J and 1K). LDHA protein expression was similarly decreased (Figure 1L and 1M). In addition, RNA sequencing analysis of HCAECs after 24 hours of IFN-γ exposure was notable for suppression of the expression of the majority of the glycolytic enzymes (Figure 1N), further supporting the conclusion that IFN-γ interferes with endothelial glucose metabolism at the level of transcription (Figure 1O).

IFN-γ Accelerates Tryptophan Catabolism Resulting in an Intracellular Kynurenine Surge in HCAECs

Given the significant alterations in endothelial glucose metabolism induced by IFN-γ, we next sought to obtain a more global assessment of the landscape of different cellular metabolic pathways by targeted liquid chromatography mass spectrometry analysis of 144 common intracellular metabolites extracted from HCAECs treated with IFN-γ for 24 hours in vitro (Figure 2A). We observed a decrease in intracellular tryptophan by up to 78% (P<0.0001) (Figure 2B) after 24 hours of IFN-γ exposure with robust antiparallel accumulation of kynurenine (the first major stable metabolite of tryptophan catabolism) by 720% compared with untreated control (P<0.0001) (Figure 2C). We also observed concomitant increases in mRNA and protein expression of IDO1, an IFN-γ–activated enzyme catalyzing tryptophan degradation to kynurenine (Figure 2D and 2E). Increasing 1DO1 activity over time was suggested by a time-dependent increase in the intracellular kynurenine-to-tryptophan ratio (Figure 2F). These findings are consistent with previous reports of tryptophan depletion in noncoronary artery endothelial cells on IFN-γ exposure.[12–14]

To understand better the functional consequences of tryptophan depletion on endothelial cells, confluent HCAECs were incubated in DMEM deficient in tryptophan with or without exogenous tryptophan supplementation for 24 hours followed by assessment of changes in endothelial adhesion molecule expression and migratory capacity. Exposure to the tryptophan-deficient medium resulted in a proinflammatory phenotype with robust upregulation of intercellular adhesion molecule (P=0.0005) and vascular cell adhesion molecule (P=0.0083) gene expression (Figure 2G and 2H) and a significant impairment in HCAEC migratory capacity after mechanical (scratch) injury to the endothelial monolayer (Figure 2I and Figure S2).

IFN-γ Activates AHR and Promotes Its Dimerization With AHR Nuclear Translocator/HIF1β With a Concomitant Decrease in Nuclear HIF1α

Kynurenine is an endogenous ligand for the intracellular transcription factor AHR.[15] On ligand- and nonligand-specific activation, AHR translocates to the nucleus, dimerizes with aryl hydrocarbon receptor nuclear translocator (ARNT)/HIF1β (henceforth referred to as ARNT), and binds to the xenobiotic response element (also known as the dioxin response element) to regulate downstream target gene transcription.[16] After IFN-γ treatment and the subsequent intracellular kynurenine surge in HCAECs, we detected an increase in AHR protein expression in endothelial nuclei and nuclear extracts (Figure 3A–3C). This increase in nuclear AHR was accompanied by downstream transcriptional activation of its canonical target genes, such as *CYP1B1* (cytochrome P450 family 1 subfamily B member 1) with a >27-fold change in its mRNA expression (Figure 3D). Given that ARNT is a shared binding partner for AHR and HIF1α and necessary for their stabilization and activity as transcription factors,[17,18] we hypothesized that AHR activation and nuclear translocation by the IFN-γ–induced kynurenine increase leads to sequestration of the limited nuclear ARNT and, as a consequence, destabilizes residual HIF1α in normoxia (Figure 3H). Such competition between HIF1α and AHR (activated by an exogenous agonist) has been demonstrated in other endothelial cell types in hypoxia.[19] We further hypothesized that this mechanism likely would explain IFN-γ–induced transcriptional suppression of *SLC2A1* and *LDHA* expression—both well-characterized HIF1 target genes—as well as decreases in the expression of other glycolytic enzymes. We found that IFN-γ treatment of HCAECs for 38 hours in normoxia resulted in significant HIF1α destabilization with a 29% decrease in total nuclear protein expression (P=0.012), whereas total nuclear ARNT remained unchanged (Figure 3C). A similar and significant decrease in nuclear HIF1α was

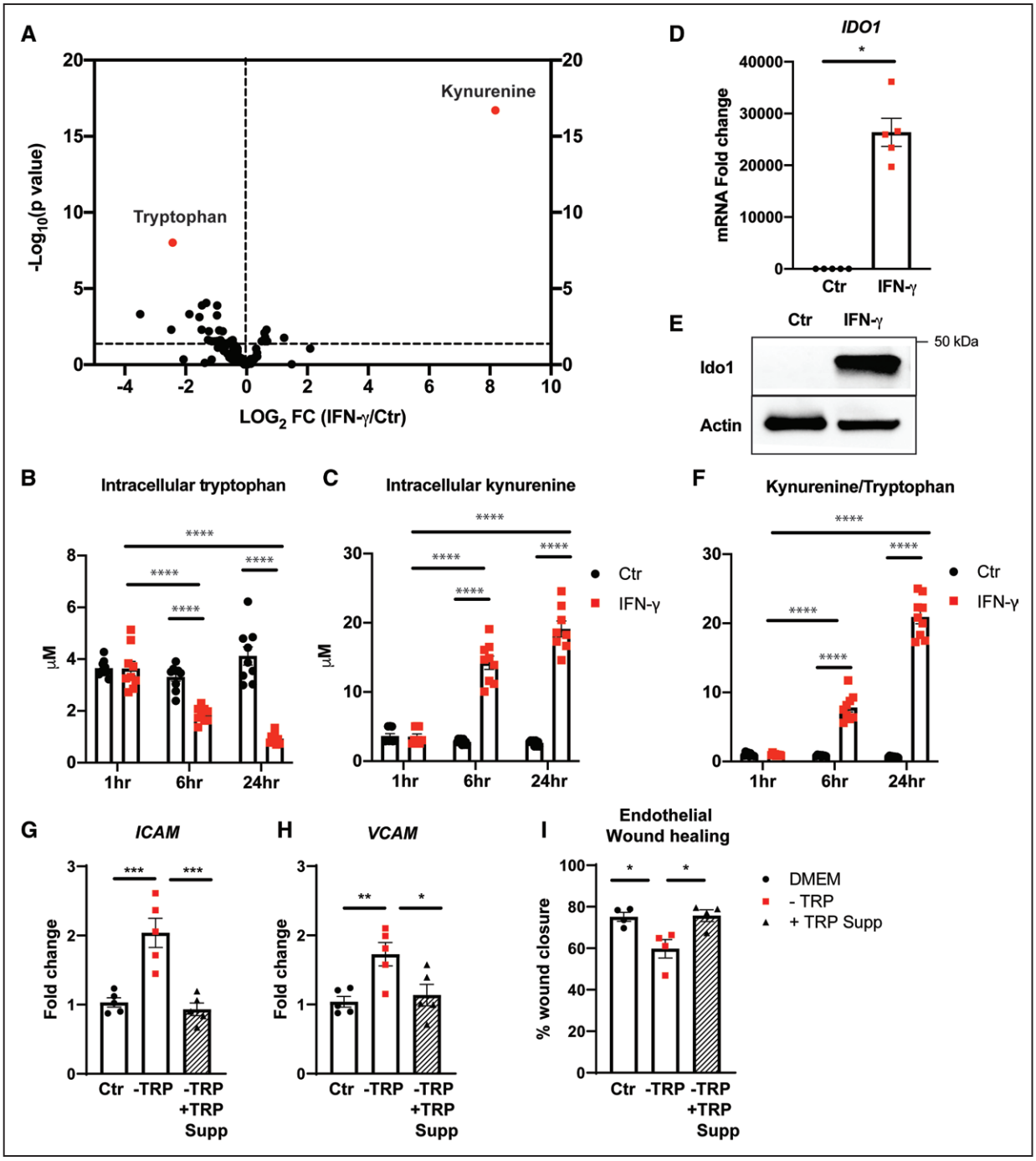

Figure 2. IFN-γ accelerates tryptophan degradation to kynurenine in HCAECs.
A, Targeted LC-MS analysis of 144 common intracellular metabolites. Log_2 of fold changes (FC) in intracellular metabolites extracted from human coronary artery endothelial cells (HCAECs) after 24 hours of IFN-γ at 50 ng/mL are depicted on the *x* axis with their *P* values on the *y* axis. Mean from 3 independent experiments. **B** and **C**, Intracellular tryptophan (**B**) and kynurenine (**C**) in HCAECs measured by LC-MS after 1, 6, and 24 hours of IFN-γ treatment. Mean±SEM from 9 biological replicates from 3 independent experiments. **D**, *IDO1* mRNA expression fold change in HCAECs after the same IFN-γ treatment. Mean±SEM from 3 independent experiments. **E**, IDO1 protein expression changes in HCAECs after the same IFN-γ treatment. Representative Western blot. **F**, Intracellular kynurenine/tryptophan ratio over time indicating increased IDO1 activity. Mean±SEM from 9 biological replicates from 3 independent experiments. **G** and **H**, Adhesion molecules, *ICAM* (**G**) and *VCAM* (**H**), mRNA expression fold changes in HCAECs measured by real-time PCR after 24 hours incubation in control DMEM (Ctrl) or DMEM deficient in tryptophan (-TRP) with (black triangles with hatched bars) or without (red squares) TRP supplementation (-TRP + TRP Supp). Mean±SEM from 3 independent experiments. **I**, Percentages of wound closure of monolayer re-endothelialization after 24 hours incubation in the above medium calculated by the following formula: [(open area at 0 hours) – (open area at 48 hours)]/(open area at 0 hours) × 100. Mean±SEM from 4 independent experiments. Statistical significance was determined by 2-way ANOVA with post hoc Tukey multiple comparisons test (**B**, **C**, and **F**), Welch *t* test (**D**), or 1-way ANOVA with post hoc Bonferroni pairwise comparison test (**G**–**I**). ICAM indicates intercellular adhesion molecule; IDO1, indoleamine 2,3,-dioxygenase 1; IFN, interferon; LC-MS, liquid chromatography mass spectrometry; and VCAM, vascular cell adhesion molecule. **P*<0.05; ***P*<0.01; ****P*<0.001; *****P*<0.0001.

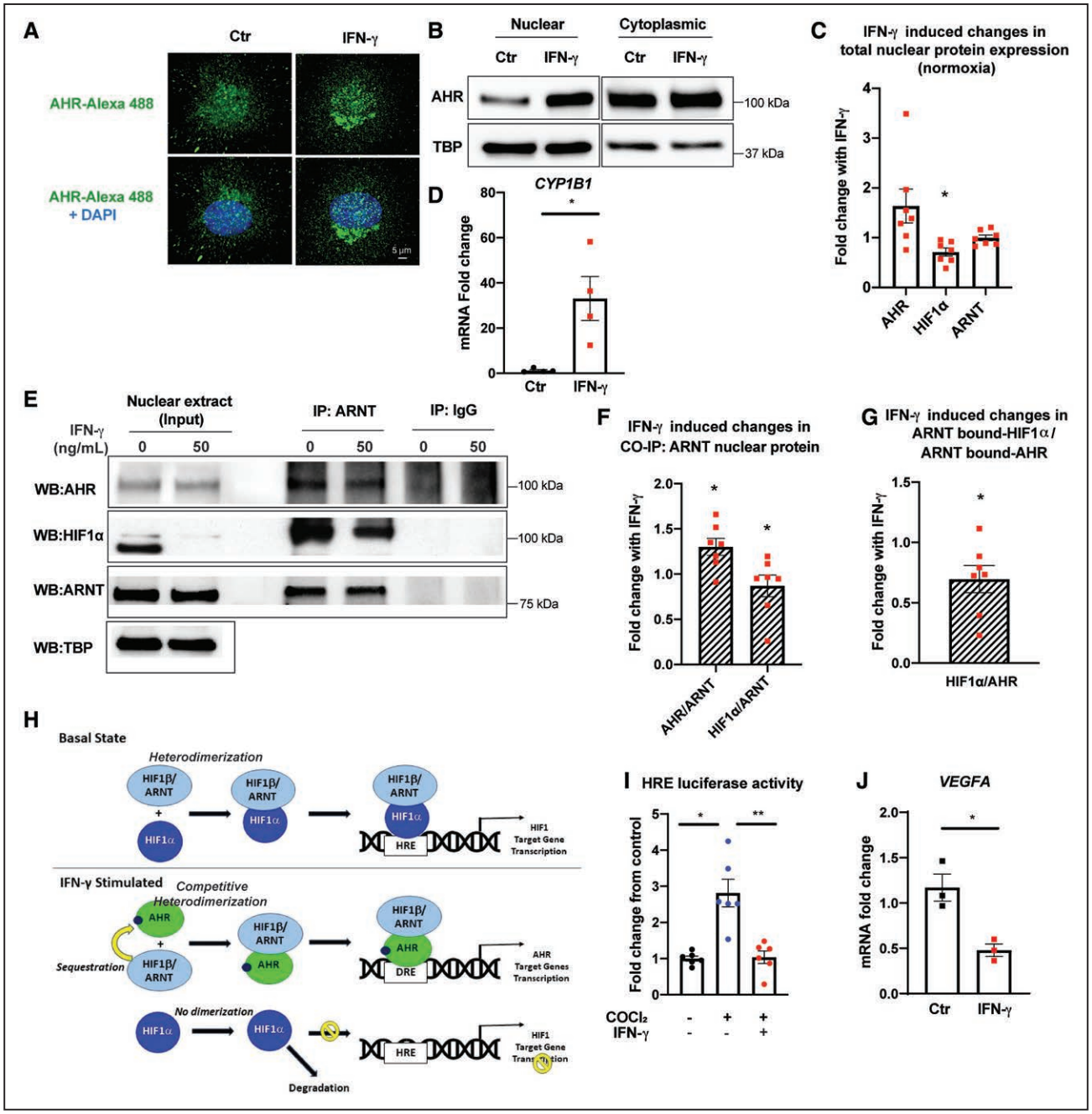

Figure 3. IFN-γ results in AHR activation, nuclear translocation, dimerization with ARNT, and transcriptional activation of its target gene and concomitantly decreases total nuclear HIF1α in HCAECs.

A, Confocal microscopy analysis of intracellular AHR (green, Alexa Fluor 488) superimposed with DAPI nuclei as staining (blue) after 24 hours of IFN-γ treatment at 50 ng/mL. Representative images. **B**, Protein expression of AHR in the nuclear and cytoplasmic extracts after IFN-γ treatment. Representative Western blots. **C**, IFN-γ–induced fold changes in total nuclear protein expression levels of AHR, HIF1α, and ARNT in HCAECs after 38 hours of IFN-γ treatment in normoxia. Densitometric quantification of each protein level was normalized by loading control protein, TATA binding protein (TBP), before the IFN-γ–treated group was compared with the untreated control within each experiment. Mean±SEM from 7 independent experiments. AHR, fold change (FC) 1.64; *P*=0.11. HIF1α, FC 0.71; *P*=0.012. ARNT, FC 1.0; *P*=0.97. **D**, Transcriptional activation of a canonical AHR target gene *CYP1B1* by quantitative polymerase chain reaction by IFN-γ. Mean±SEM from 3 independent experiments. **E**, Nuclear protein extracts of human coronary artery endothelial cells (HCAECs) were coimmunoprecipitated (CO-IP) with ARNT after IFN-γ treatment and probed with antibodies against AHR, HIF1α, and ARNT. **Left**, Protein detection in the 8% of the total unprocessed nuclear lysates (input) used for each CO-IP experiment. Representative Western blot. **F**, IFN-γ–induced fold changes in nuclear AHR and HIF1α coimmunoprecipitated with ARNT in normoxia. Densitometric quantification of each protein was normalized by the coimmunoprecipitated ARNT level before the IFN-γ–treated group was compared with the untreated control within each experiment. Mean±SEM from 7 independent experiments. IP ARNT, AHR FC 1.30; *P*=0.018. IP ARNT, HIF1α FC 0.86; *P*=0.036. **G**, Fold changes in the relative abundance of ARNT-bound nuclear HIF1α over ARNT-bound AHR in HCAECs after IFN-γ treatment over untreated control, *P*=0.036. Mean±SEM from 7 independent experiments. **H**, Schematic summary of the proposed mechanism. (*Continued*)

Figure 3 Continued. I, HRE luciferase activity after 48 hours cobalt chloride ($CoCl_2$) treatment with or without IFN-γ. HRE firefly luciferase activity was normalized by the cotransfected *Renilla* luciferase activity in each sample before quantifying the fold changes in the reporter activity from the untreated control group. Mean±SEM from 3 independent experiments. **J**, Transcriptional suppression of a canonical HIF1 target gene *VEGFA* by quantitative polymerase chain reaction by IFN-γ. Mean±SEM from 3 independent experiments. Statistical significance was determined by 1-sample *t* test (**C, F,** and **G**), Welch *t* test (**D**), Welch ANOVA with post hoc Dunnett T3 multiple comparisons test (**I**), and unpaired 2-tailed Student *t* test (**J**). AHR indicates aryl hydrocarbon receptor; ARNT, aryl hydrocarbon receptor nuclear translocator; Ctr, control; CYP1B1, cytochrome P450 family 1 subfamily B member 1; DAPI, 4'6-diamidino-2-phenylindole; DRE, digoxin responsive element; HIF1α, hypoxia-inducible factor 1 α; HRE, hypoxia-responsive element; IFN, interferon; IP, immunoprecipitation; VEGFA, vascular endothelial growth factor A; and WB, Western blot. **P*<0.05; ***P*<0.01.

noted with IFN-γ treatment in hypoxia (1% O_2), although the extent of HIF1α destabilization was somewhat less (17%) (data not shown). Coimmunoprecipitation analysis (Figure 3E–3G) comparing the relative quantities of ARNT-bound HIF1α and ARNT-bound AHR in nuclear extracts after the same IFN-γ exposure showed a 30% decrease in ARNT-bound HIF1α/ARNT-bound AHR when compared with untreated controls (*P*=0.036). Consistent with the decreased nuclear HIF1α availability by IFN-γ, IFN-γ abrogated cobalt chloride–induced hypoxia-responsive element–luciferase reporter activity in HCAECs (Figure 3I) and suppressed another canonical HIF1 target gene expression, *VEGFA*, by >50% (Figure 3J).

IFN-γ Exposure Results in Widespread Suppression of HIF1 Target Gene Expression in HCAECs

Downstream of IFN-γ–induced HIF1α destabilization in quiescent HCAECs in normoxia, we found global suppression of HIF1 target gene expression (Figure S3 and Table S1). In addition to the significant decreases in the expression of genes encoding almost all of the glycolytic enzymes, other markedly suppressed genes involve broad aspects of endothelial cell survival and function, including cell growth and viability, with a 51% decrease in *IGF2* (insulin-like growth factor) and its binding protein (*IGFBP*) isotypes, as well as a 22% decrease in *CDKN1* (cyclin-dependent kinase inhibitor). In addition, there were decreases in the expression of genes involved in vascular remodeling (transforming growth factor β [*TGFB*]), vasomotor tone (adrenomedullin [*ADM*], adrenoceptor α 1B [ADRA1B]), thrombosis) serpin family E member 1 [*SERPINE1*]), and heme (heme oxygenase 1 [*HMOX1*]) and iron metabolism (transferrin receptor [*TFRC*]).

IFN-γ–Induced Suppression of Endothelial Glycolytic Genes Is Mediated by IDO1-AHR-HIF1 Pathway Interactions

To link further IFN-γ–induced activation of IDO1-kynurenine-AHR pathways and concomitant HIF1α destabilization with IFN-γ–induced suppression of glycolytic enzyme gene expression, we performed a series of targeted gene silencing and pharmacological inhibition studies specific to each pathway. Pharmacological inhibition of IDO1 by 1-methyltryptophan abrogated IFN-γ–induced suppression of *SLC2A1* gene expression (Figure 4A) and partially attenuated suppression of *LDHA* (Figure 4B) in HCAECs. Similarly, gene silencing of *AHR* attenuated IFN-γ–induced suppression of *LDHA* gene expression (Figure 4C and 4D and Figure S4). Last, silencing of the von Hippel-Lindau tumor suppressor gene (*VHL*)[20] successfully stabilized nuclear HIF1α protein expression in normoxia (Figure 4E) beyond that of the control siRNA-treated sample and abrogated the IFN-γ–induced suppression of *LDHA* gene expression (Figure 4F and 4G and Figure S4 and Tables S2 and S3).

IFN-γ Depletes Basal Intracellular NAD(H) in HCAECs

Oxidized NAD (NAD^+) and total NAD(H) are essential elements of cellular bioenergetics and redox homeostasis, serving not only as cofactors for glycolysis but also as important regulators of glycolysis and intracellular signaling (see review[21]). IFN-γ exposure resulted in a significant dose-dependent depletion of intracellular NAD(H) by 20% (*P*=0.0078) without a significant change in the NAD^+/NADH ratio (Figure 5A and 5B). These findings were contrary to our initial expectation that the IFN-γ–induced intracellular kynurenine surge would promote de novo NAD^+ synthesis and increase total intracellular NAD(H). Pretreatment of HCAECs with 3-aminobenzamide, an inhibitor of PARP, completely prevented IFN-γ–induced depletion of intracellular NAD(H) (Figure 5A), suggesting such NAD^+ depletion is primarily driven by PARP activation. Of note, no significant differences in cell viability were noted between the IFN-γ–treated cells and untreated controls. Supplementation with the NAD^+ precursor, nicotinamide mononucleotide, also effectively restored the intracellular NAD(H) level after IFN-γ exposure (Figure 5C).

With marked impairment of glycolysis and NAD(H) depletion, we next hypothesized that total intracellular energy balance would be impaired. It is interesting that ATP/ADP and ATP/AMP ratios were unchanged with IFN-γ (Figure 5D and 5E), raising a question about the nature of alternative metabolic pathways and energy source(s) that compensate for impaired glycolysis.

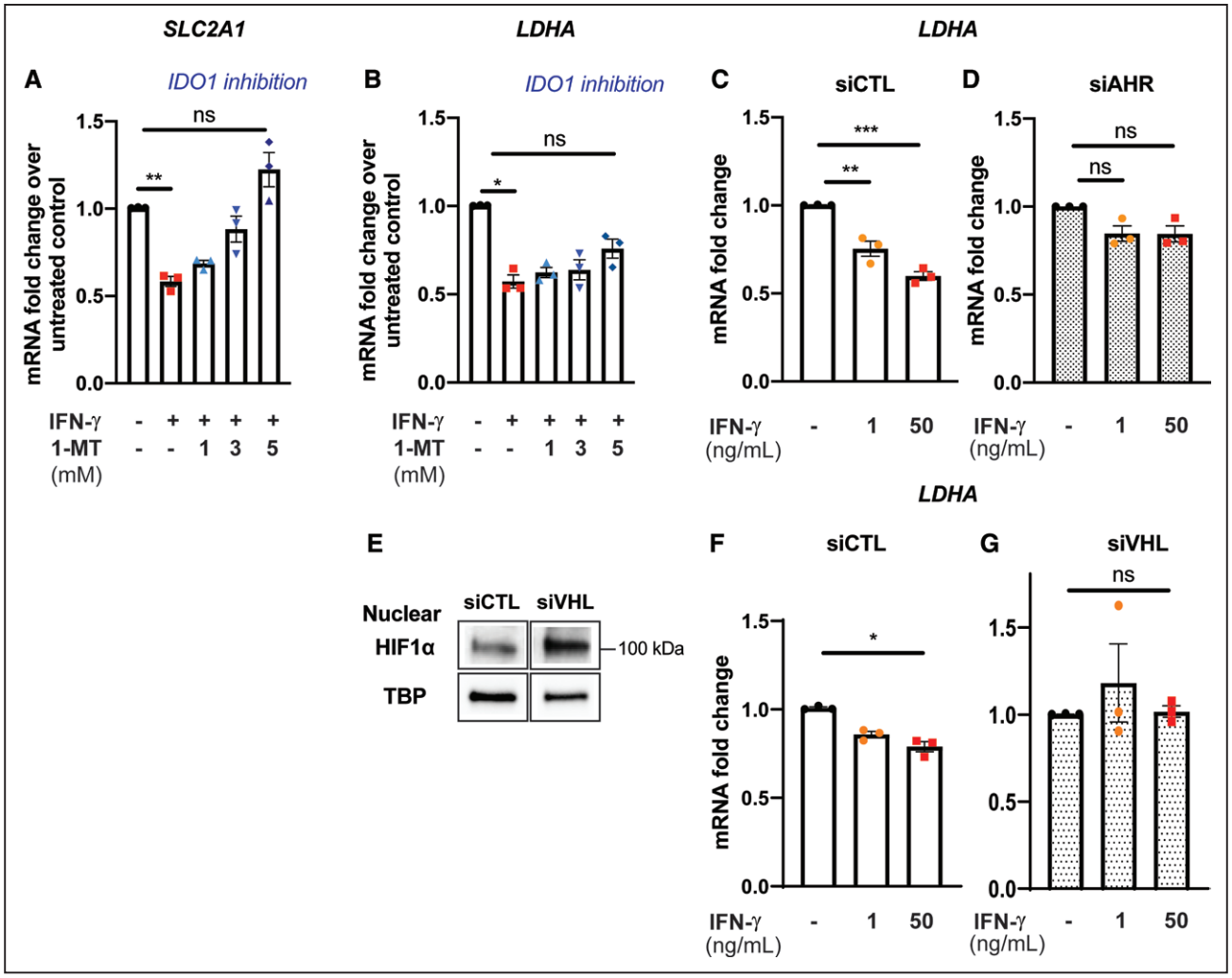

Figure 4. IFN-γ–induced suppression of glycolytic gene expression is mediated by the interactions between the IDO1-AHR-HIF1 transcriptional regulatory pathways.

A and **B**, Pharmacological inhibition of indoleamine 2,3,-dioxygenase 1 (IDO1) by 1-methyltryptophan (1-MT) abrogates IFN-γ–induced suppression of *SLC2A1* gene expression (**A**) and partially attenuates suppression of *LDHA* (**B**) in human coronary artery endothelial cells (HCAECs). Data represent mean±SEM from 3 independent experiments. **C** and **D**, Gene silencing of AHR attenuates IFN-γ–induced suppression of *LDHA* gene expression in HCAECs. Data represent mean mRNA fold changes with IFN-γ treatment compared with those not exposed to IFN-γ within each siRNA treatment group ±SEM from 3 independent experiments. **E**, Gene silencing of von Hippel-Lindau tumor suppressor (VHL) stabilizes nuclear HIF1α protein expression in normoxia. TATA binding protein (TBP) was used as a loading control. Representative Western blot. **F** and **G**, HIF1α stabilization in normoxia by gene silencing of VHL abrogates IFN-γ–induced suppression of *LDHA* gene expression in HCAECs. Data represent mean mRNA fold changes with IFN-γ treatment compared with those not exposed to IFN-γ within each siRNA treatment group ±SEM from 3 independent experiments. Statistical significance was determined by 1-way ANOVA with post hoc Tukey multiple comparisons test (**A**–**D**) or Kruskal-Wallis test with post hoc Dunn multiple comparisons test (**F** and **G**). AHR indicates aryl hydrocarbon receptor; CTL, control; HIF1α, hypoxia-inducible factor 1 α; IFN, interferon; LDHA, lactate dehydrogenase A; ns, not significant; and SLC2A1, solute carrier family 2 member 1. **P*<0.05; ***P*<0.01; ****P*<0.001.

IFN-γ Results in Endothelial Metabolic Reprogramming to Augment FAO

Indeed, despite the inhibition of glycolysis by IFN-γ resulting in a marked depletion of intracellular pyruvate (Figure 1I), a 23% increase in basal mitochondrial oxygen consumption rate (OCR) or oxidative phosphorylation (defined as [basal OCR] – [OCR after antimycin A and rotenone injection]) was noted with IFN-γ (*P*=0.0032; Figure 6A). This finding was independent of the presence of serum or growth factor supplementation in the basal medium (Figure S1B and S1C). Furthermore, there was a 30% increase in mitochondrial respiration associated with ATP production (ATP-linked OCR, defined as [basal OCR] – [OCR after oligomycin injection]; *P*=0.0021) (Figure 6B). Overall, there was a significant shift away from glycolysis to oxidative phosphorylation in basal endothelial metabolism after IFN-γ exposure as demonstrated by an increased basal mitochondrial OCR–to–extracellular acidification rate ratio (Figure 6C) and a left and upward shift in the representative extracellular acidification rate–OCR plot (Figure 6D). This

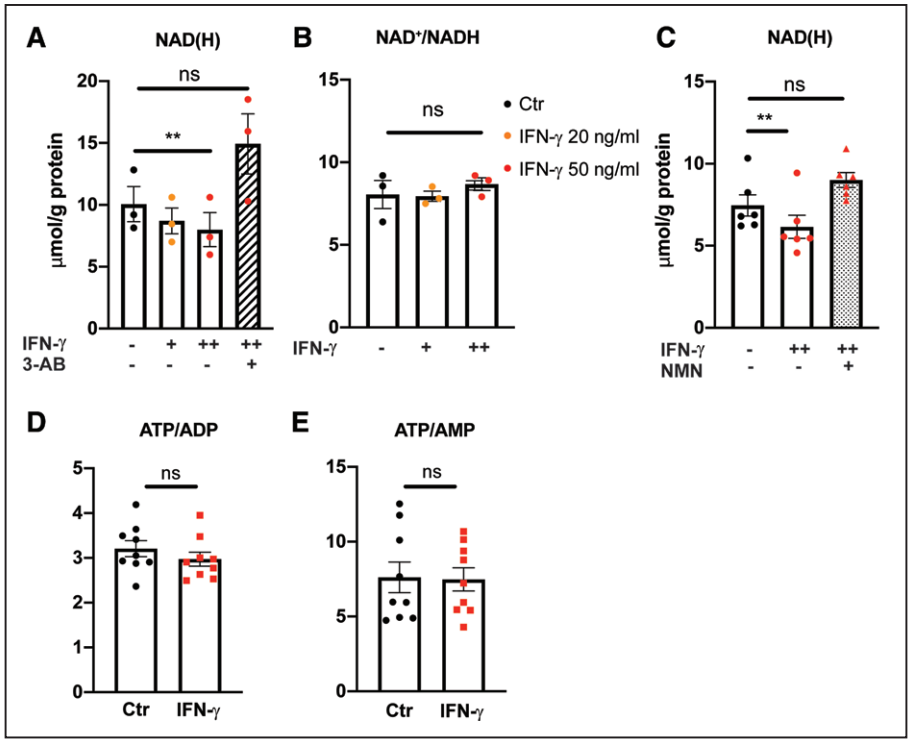

Figure 5. IFN-γ exposure depletes basal intracellular NAD(H) by increased ADP-ribosylation in HCAECs.
A, Intracellular NAD(H) (total NAD^+ and NADH) in human coronary artery endothelial cells (HCAECs) after IFN-γ treatment for 24 hours at 20 or 50 ng/mL detected by bioluminescent assay with or without 1-hour pretreatment with a poly (ADP-ribose) polymerase inhibitor, 3 aminobenzamide (3-AB). **B**, Intracellular NAD^+/NADH ratio after the same IFN-γ treatments. **C**, Intracellular NAD(H) in HCAECs after IFN-γ treatment for 24 hours at 50 ng/mL with or without subsequent nicotinamide mononucleotide (NMN) supplementation at 0.5 mM for an additional 24 hours. Data represent mean±SEM from 3 independent experiments. **D** and **E**, Intracellular ATP/ADP (**D**) and ATP/AMP (**E**) ratios in HCAEC after 24 hours of IFN-γ treatment measured by HPLC. Data represent mean±SEM from 9 independent experiments. Statistical significance was assessed using 1-way ANOVA with post hoc Tukey multiple comparisons (**A**–**C**) or an unpaired 2-tailed Student *t* test (**D** and **E**). Ctr indicates control; HPLC, high performance liquid chromatography; IFN, interferon; NAD(H), nicotinamide adenine dinucleotide; and ns, not significant. $^{**}P<0.01$.

finding raised the important issue of the identity of the alternative fuel source(s) that supplies the mitochondrial electron transport chain in the face of impaired glucose metabolism.

In contrast with the global transcriptional suppression of glycolytic enzymes by IFN-γ (Figure 1N), gene expression levels of multiple key enzymes regulating FAO were significantly elevated in HCAECs treated with IFN-γ (Figure 6E). These included up to a 450% increase in acyl-CoA synthetase long-chain family members expression as well as a 57% increase in acyl-CoA dehydrogenase medium-chain expression. For an activated cytosolic long-chain fatty acid to cross the mitochondrial inner membrane for oxidation, transfer of its acyl moiety to carnitine (acyl-carnitine) by CPT1 (carnitine palmitoyl transferase 1) is required. Once in the mitochondrial matrix, the acyl group of the fatty acid is transferred to CoA (fatty acyl-CoA), which is subsequently oxidized to generate ATP. There was a 47% decrease in intracellular butyrylcarnitine, an acyl-carnitine, in IFN-γ–treated HCAECs, as well as a similarly decreasing trend in propionylcarnitine (Figure 6F and 6G). Together with the transcriptional activation of multiple FAO enzymes, such a decrease in precursors to fatty acyl-CoAs was consistent with increased FAO in IFN-γ–treated HCAECs. This metabolic shift from glycolysis to FAO was accompanied by earlier activation of AMP-activated protein kinase by IFN-γ (Figure 6H and 6I).

With pharmacological inhibition of CPT1 (etomoxir), the rate-limiting FAO enzyme, IFN-γ–treated HCAECs could no longer augment basal oxidative phosphorylation (Figure 6J) or ATP-linked mitochondrial OCR (Figure 6K). Similarly, gene silencing of *CPT1A* attenuated the IFN-γ–induced increase in oxidative phosphorylation (Figure S5A–S5C).

Furthermore, inhibition of FAO disrupted intracellular energy balance in IFN-γ–treated cells as noted by >20% reduction in the ATP/ADP ratio (Figure 6L and 6M), supporting the novel role of FAO in maintaining endothelial intracellular energy balance in the face of IFN-γ–induced impaired glucose metabolism. Of note, no transcriptional activation of the enzymes involved in glutaminolysis or significant changes in intracellular glutamine or glutamate levels were observed with IFN-γ treatment (Figure S5D–S5F), eliminating this amino acid pathway from consideration as an alternate energy source.

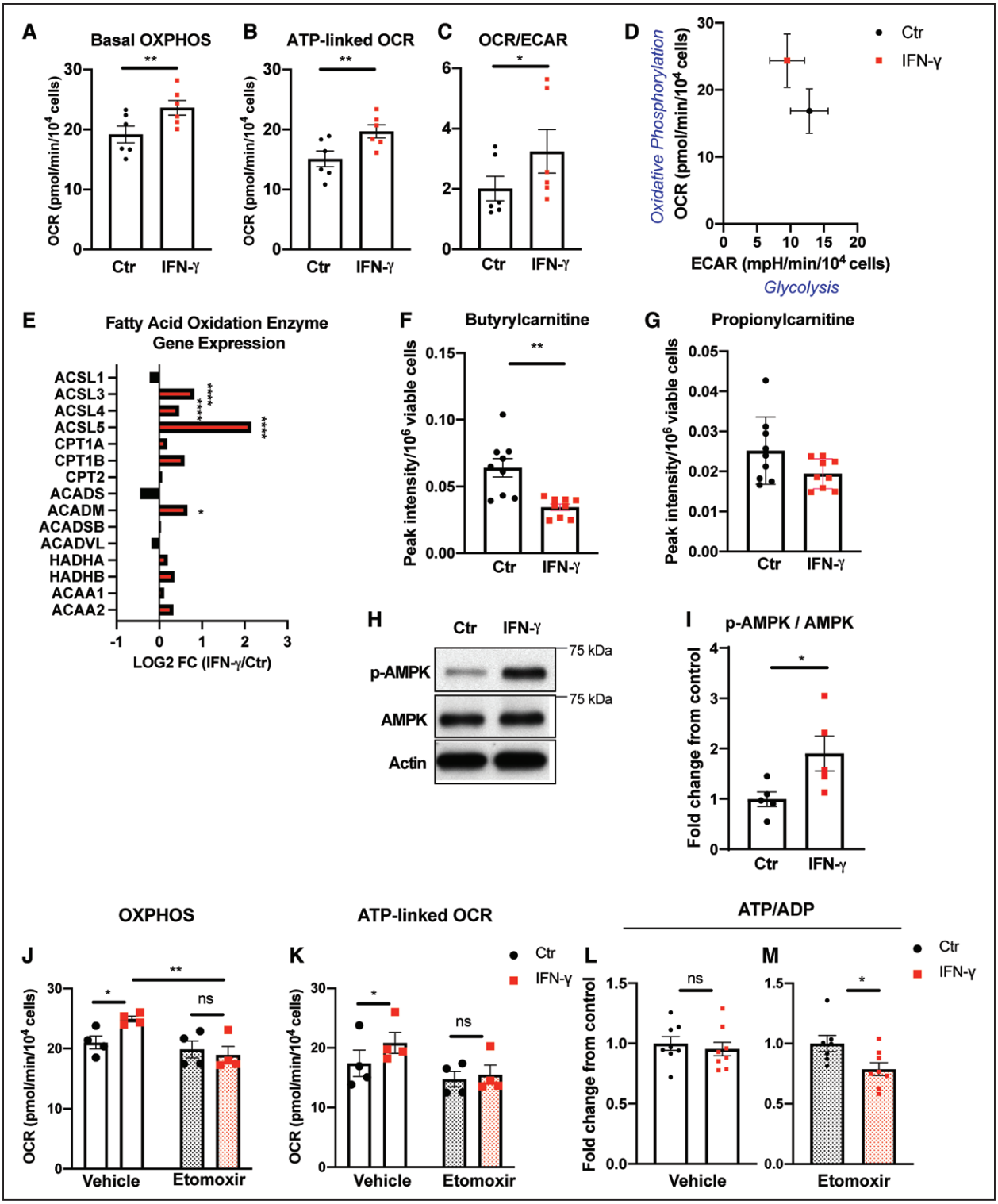

Figure 6. IFN-γ activates fatty acid oxidation in HCAECs.

A, Real-time extracellular flux analysis of mitochondrial oxygen consumption rate reflecting oxidative phosphorylation (OXPHOS) of human coronary artery endothelial cells (HCAECs) after IFN-γ treatment at 50 ng/mL for 24 hours. **B**, Mitochondrial oxygen consumption associated with ATP production from the same experiments. **C**, IFN-γ–induced changes in the ratio between mitochondrial oxygen consumption rate (OCR) and extracellular acidification rate (ECAR) representing decreased glycolysis and increased OXPHOS in HCAECs. Mean±SEM from 6 independent experiments (**A**–**C**). Statistical significance was assessed using paired 2-tailed Student *t* tests (**A** and **B**) or Wilcoxon matched-pairs signed-rank test (**C**). **D**, Representative plot demonstrating altered basal glycolysis and oxidative phosphorylation activities in HCAECs after the same IFN-γ treatment in a single experiment. Mean±SEM from 9 or 10 biological replicates. **E**, IFN-γ induces gene expression changes in the fatty acid oxidation enzymes by RNA sequencing analysis of HCAECs obtained in biological triplicates. Statistical significance was determined on the basis of the *P* values adjusted for multiple test hypotheses by the Benjamini-Hochberg procedure. (*Continued*)

Figure 6 Continued. F and **G**, Intracellular acylcarnitines (butyrylcarnitine [**F**] and propionylcarnitine [**G**]) in HCAECs measured by LC-MS after the same IFN-γ treatment. Mean±SEM of 9 biological replicates from 3 independent experiments. Statistical significance was assessed using Welch *t* test. **H** and **I**, Phosphorylation of AMP-activated protein kinase (AMPK) at Thr 172 after 7 hours of IFN-γ treatment at 50 ng/mL. Representative Western blot (**H**) and densitometric analysis (**I**). Mean±SEM from 3 independent experiments analyzed by 2-tailed Student *t* test. **J**, Real-time extracellular flux analysis of basal OXPHOS of HCAECs after the same IFN-γ treatment with and without 1-hour 10 μM etomoxir incubation just before analysis. **K**, Mitochondrial oxygen consumption associated with ATP production from the same experiments. Mean±SEM from 4 independent experiments (**J** and **K**). Statistical significance was assessed by 2-way ANOVA with Sidak multiple comparison tests. **L** and **M**, Intracellular ATP/ADP ratios detected in HCAECs after the IFN-γ treatment with (**M**) and without (**L**) etomoxir. Data represent mean fold changes with IFN-γ treatment compared with those not exposed to IFN-γ within each inhibitor treatment group ±SEM from 7 to 9 independent experiments. Statistical significance was assessed using a 2-tailed Student *t* test. ACAA indicates acetyl-CoA acyltransferase; ACADM, acyl-CoA dehydrogenase medium chain; ACADS, acyl-CoA dehydrogenase short chain; ACADSB, acyl-CoA dehydrogenase short/branched chain; ACADVL, acyl-CoA dehydrogenase very long chain; ACSL, acyl-CoA synthetase long-chain family member; CPT, carnitine palmitoyl transferase; Ctr, control; FC, fold changes; HADH, hydroxyacyl-CoA dehydrogenase trifunctional multienzyme complex; IFN, interferon; LC-MS, liquid chromatography mass spectrometry; and ns, not significant. **P*<0.05; ***P*<0.01; *****P*<0.0001.

IFN-γ Exposure Depletes Basal Endothelial cGMP and Impairs Endothelial Proliferative and Migratory Capacity

Metabolic derangements induced by IFN-γ treatment were accompanied by unfavorable phenotypic changes in HCAECs. Endothelial dysfunction in association with cGMP-NO insufficiency has been well established as an important correlate of heightened cardiovascular risk[22] and deemed a precursor to coronary artery atherogenesis.[23] Twenty-five hours of IFN-γ exposure at 50 ng/mL resulted in a 29% reduction in basal intracellular cGMP in HCAECs (*P*=0.0247; Figure 7A and 7B). This reduction was observed despite increased phosphorylation of the serine 1177 residue of endothelial NO synthase (Figure S6A–S6D), consistent with recent examples of discordance between endothelial NO synthase phosphorylation in human umbilical vein endothelial cells and NO formation.[24] Total endothelial NO synthase protein expression did not change (Figure S6E–S6F).

Similar to the effect of tryptophan depletion (Figure 2I and Figure S2), 30 hours of IFN-γ exposure resulted in impaired healing of an endothelial monolayer after mechanical (scratch) injury, a process dependent on endothelial proliferative and migratory function (*P*=0.0098; Figure 7C–7G) and consistent with previous reports of the antiangiogenic effect of IFN-γ.[25]

DISCUSSION

In the present study, IFN-γ impaired coronary artery endothelial glucose metabolism by glycolysis inhibition—by accelerated tryptophan catabolism—and NAD(H) depletion while activating fatty acid oxidation. Without FAO upregulation, IFN-γ–exposed HCAECs suffered a significant intracellular energy deficit, which highlights the novel role of endothelial FAO in preserving overall intracellular energy balance in the face of T cell–mediated endothelial metabolic derangements induced by this cytokine. These metabolic changes were associated with pathological endothelial phenotypic changes, including intracellular cGMP depletion and impaired migration and proliferation. To the best of our knowledge, this is the first report of the metabolic shift from glucose use to FAO in any cell type induced by IFN-γ, a major cytokine in human atheroma, as well as in antiviral, antitumor, and autoimmune milieux.

Studies have established glycolysis as essential for endothelial survival, proliferation, and angiogenesis.[6,26] Although studies linking impaired glycolysis with vascular pathologies centered on the inhibition or insufficiency of specific glycolytic regulators, especially PFKFB3 (gene encoding 6-phosphofructo-2-kinase/fructose-2,6-biphosphatase),[5,6] IFN-γ treatment of quiescent HCAECs in normoxia in the present study resulted in a far more extensive (global) suppression of nearly all glycolytic enzymes at the transcriptional level with a correlative decline in associated intracellular metabolites. Suppression of glycolysis by IFN-γ was specific to endothelial cells, in striking contrast to their neighboring macrophages in atheroma in which IFN-γ promotes glycolysis and a switch to a proinflammatory phenotype.[27] To the best of our knowledge, the only other biological context wherein IFN-γ resulted in a similar directional change in glycolysis as in endothelial cells involves *Chlamydia trachomatis*–infected epithelial cell lines.[28]

The role of HIF as a major regulator of endothelial function and metabolism has been established first in hypoxia,[29–31] with now growing appreciation of its role in normoxia.[32–34] The biological consequences of IFN-γ–induced loss of tonic HIF activity in diseased and nondiseased endothelial cells are likely system-wide—well beyond its implications in atherogenesis[35–37]—either as a direct sequela of disrupted glucose metabolism or by impaired transcriptional activation of the multitude of genes governing important aspects of endothelial function (Figure S3). It is also important to note that endothelial glucose metabolism is regulated by closely intertwined networks of numerous transcription factors and signaling pathways in addition to HIF, including, but not limited to, MYC (MYC proto-oncogene, bHLH transcription factor), mTOR (mammalian targets of rapamycin), AMP-activated protein kinase, KLF (Kruppel-like factors), and their interactions.[1]

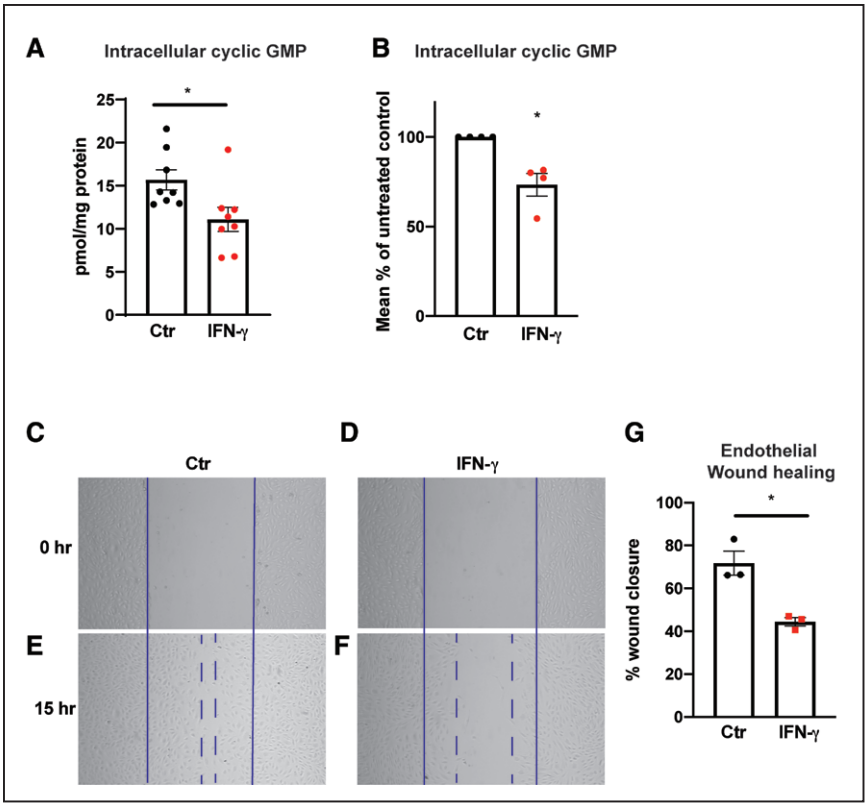

Figure 7. IFN-γ exposure depletes endothelial basal intracellular cGMP and impairs proliferation and migratory capacity.
A and **B**, Intracellular cGMP levels from human coronary artery endothelial cells (HCAECs) quantified using ELISA after 25 hours of IFN-γ treatment at 50 ng/mL. Absolute intracellular cGMP measurements normalized to total protein/plate (pmol/mg protein) (**A**) and relative intracellular cGMP levels expressed as the percentages of those of untreated control groups (**B**). Mean±SEM from 8 biological replicates from 4 independent experiments. **C** through **F**, HCAEC proliferation and migration capacities were assessed by scratch assay after IFN-γ exposure for 30 hours. Representative bright-field images are shown at 0 hours (**C** and **D**) and 15 hours after the scratch (**E** and **F**). **G**, Percentages of wound closure or monolayer re-endothelialization after IFN-γ treatment were calculated by the following formula: [(open area at 0 hours) − (open area at 15 hours)]/(open area at 0 hours) × 100. Mean±SEM from 3 independent experiments. Statistical significance was assessed using a 2-tailed Student *t* test (**A** and **G**) or 1-sample *t* test (**B**). Ctr indicates control; and IFN, interferon. *$P<0.05$.

Maintenance of intracellular NAD(H) balance is tightly regulated and indispensable for cellular bioenergetics. Despite robust activation of the rate-limiting step for de novo NAD^+ synthesis, IFN-γ resulted in a net 20% depletion in total intracellular NAD(H) driven primarily by PARP activation by IFN-γ, similar to that observed in cancer cell lines[38] and peripheral blood mononuclear cells.[39] Although IFN-γ–induced cellular apoptosis has been reported in various biological contexts, the exact mechanism by which IFN-γ induces PARP activation remains incompletely understood. The consequences of NAD^+ depletion in relation to glucose metabolism are severalfold. In addition to creating cofactor deficiency for multiple glycolytic enzymes, NAD^+, depletion alone can result in PARP activation,[40] which, in turn, can inhibit glycolysis further independent of NAD^+ by PARPylation of HK1.[41,42] In the present study, pretreatment of HCAECs with a PARP inhibitor blocked IFN-γ–mediated NAD^+ depletion, suggesting that the increased PARP activity was driven by IFN-γ first and was not a mere consequence of the NAD^+ depletion that ensued. The current study highlights a PARP-mediated degradation mechanism, but it is worth noting that total intracellular NAD(H) reflects the summation and complex cross-regulation of major NAD^+ biosynthesis and degradation pathways (see review[21]), as demonstrated by our ability to restore intracellular NAD(H) by nicotinamide mononucleotide after IFN-γ exposure.

Unexpectedly, conserved intracellular ATP/ADP balance was found in this study despite a substantial impairment of glycolysis and NAD(H) loss after IFN-γ exposure. Further investigation of compensatory metabolic pathways led to the identification of novel effects of IFN-γ on endothelial FAO and a role for fatty acids in fueling ATP-coupled mitochondrial respiration. Although IFN-γ had been noted to promote adipocyte lipolysis[43] and modulate fatty acid incorporation in monocyte and macrophage membrane phospholipids,[44] its role in promoting FAO as an alternative fuel source has not been previously described.

Endothelial FAO had been known mostly for nonexergonic roles, such as cell fate,[45] proliferation and vessel sprouting,[46–48] vascular permeability,[48] nucleotide synthesis,[47] and redox homeostasis.[49] Undiminished intracellular ATP/ADP despite FAO inhibition in basal quiescent HCAECs in the present study (in the absence of IFN-γ) is consistent with the current understanding that FAO provides minimal contribution to basal endothelial energy balance.[49] More than 20% loss of the intracellular ATP/ADP resulting from acute CPT1 inhibition in IFN-γ–exposed HCAECs, however, signifies that IFN-γ–augmented endothelial FAOs contribute to overall cellular bioenergetics in the face of disrupted glucose use. Complete[50] or partial[51] extracellular glucose deprivation in culture media had been shown to increase FAO in human umbilical vein endothelial cells or bovine aortic endothelial cells, respectively. Our observation is especially intriguing because the endothelial metabolic shift from glycolysis to FAO occurred without a glucose deficit, being

purely driven by IFN-γ. We propose that IFN-γ creates a relative hypoglycemic or starvation state in the intracellular compartment in HCAECs by inhibition of glucose uptake and glycolysis, requiring that the cell resort to an alternative fuel source even with abundant extracellular glucose available. The AMP-activated protein kinase activation we observed in these cells likely contributes to facilitating this metabolic shift. The extent of intracellular ATP/ADP (21%) balance contributed by FAO in IFN-γ–treated HCAECs closely matched the 20% decrease in glycolytic activity resulting from IFN-γ. This finding illustrates the tightly regulated, yet highly fluid, crosstalk between multiple metabolic pathways coexisting within a single cell type in which perturbation in one pathway has widespread effects on others (Figure 8). The complex interplay between glycolysis and FAO has been well described in other tissues and cell types (eg, the Randle cycle)[52] but remains incompletely characterized in general and not previously studied in endothelial cells specifically.

The potential clinical implications of endothelial metabolic derangements from chronic IFN-γ exposure in atheroma rich in activated T lymphocytes in ischemic heart disease are paramount. NAD^+ depletion in other cell types has been demonstrated to result in necrotic cell death.[53] Impaired glycolysis and suppression of growth factor signaling likely inhibit collateral vessel formation as demonstrated by the significantly impaired endothelial wound-healing capacity with IFN-γ. With local ischemia in the setting of hemodynamically significant coronary artery luminal stenosis, impaired HIF stabilization by IFN-γ–mediated AHR activation would compromise essential cellular adaptive responses to hypoxia, whereas chronically increased endothelial oxygen consumption in the intima may exacerbate myocardial ischemia by oxygen "steal" during the delivery of an already limited oxygen supply. In addition to the adverse phenotypic consequences of these metabolic pathways, we report for the first time that tryptophan depletion similarly impairs the endothelial migratory capacity in vitro while switching

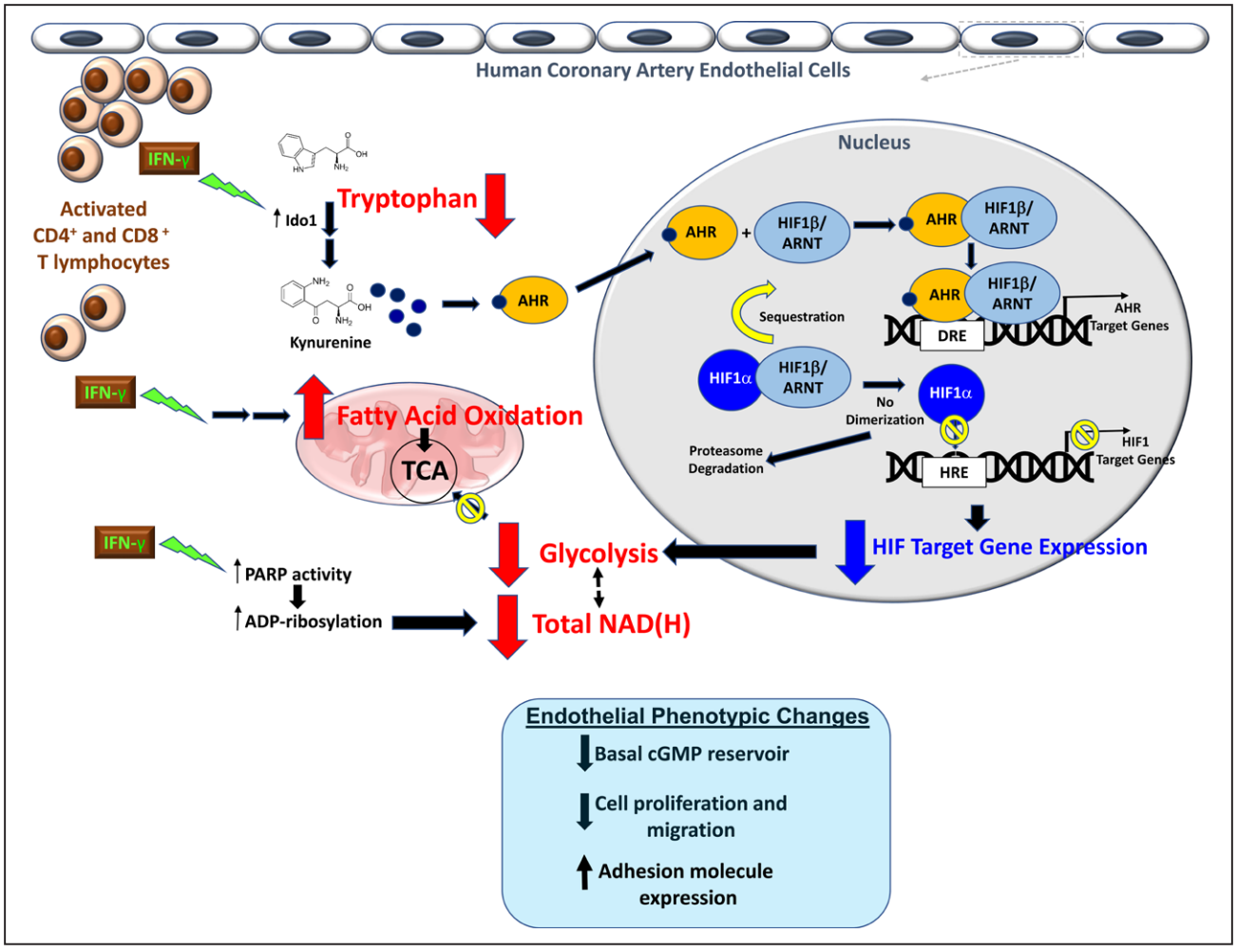

Figure 8. Proposed mechanisms for the widespread IFN-γ (interferon-γ)–induced metabolic derangements in human coronary artery endothelial cells.

AHR indicates aryl hydrocarbon receptor; ARNT, aryl hydrocarbon receptor nuclear translocator; DRE, dioxin response element; HIF1, hypoxia inducible factor 1; HRE, hypoxia response element; Ido1, indoleamine 2,3,dioxygenase 1; NAD(H), nicotinamide adenine dinucleotide; PARP, poly (ADP-ribose) polymerase; and TCA, tricarboxylic acid cycle.

HCAECs to a proinflammatory phenotype with upregulation of adhesion molecule expression as demonstrated in aortic endothelial cells.[54]

Two previous studies involving different human venous endothelial cell sources (human umbilical vein endothelial cells) have reported contrasting directional changes in intracellular cGMP levels in response to IFN-γ.[55,56] In contrast, our results in arterial endothelial cells (HCAECs) showing that IFN-γ induces a reduction in basal cGMP corroborate and provide mechanistic insight into the over 3-decades-old seminal observation linking decreased cGMP bioavailability to atheroma-laden coronary arteries.[57] It is more important to note that this significant loss of basal endothelial cGMP likely results in a system-wide disruption of key aspects of vascular homeostasis. When combined with the sequelae of the concomitant loss of tonic HIF activity and deranged metabolic balance demonstrated in this study, IFN-γ–induced endothelial cGMP depletion likely has important clinical consequences especially in the context of atherogenesis and its thrombotic and ischemic complications. Chronically decreased NO-cGMP bioavailability has been clearly associated with an increased risk for atherothrombotic diseases and adverse clinical outcomes.[22,58]

In summary, IFN-γ impairs basal glycolysis of HCAECs by activation of the IDO-kynurenine-AHR pathway resulting in decreased HIF1 activity, and depletes intracellular NAD^+ while augmenting fatty acid oxidation as an alternative fuel source (Figure 8). We propose such metabolic and phenotypic derangements resulting from pathological T lymphocyte–endothelial interaction as a fundamental mechanism linking adaptive immunity and vascular pathobiology.

ARTICLE INFORMATION

Received January 29, 2021; accepted September 23, 2021.

Affiliations

Division of Cardiovascular Medicine (L.Y.-H.L., H.H., R.W., R.M., D.E.H., J.L.) and Division of Pulmonary and Critical Care (W.M.O.), Department of Medicine, Brigham and Women's Hospital and Harvard Medical School, Boston, MA.

Acknowledgments

The authors thank Stephanie C. Tribuna for expert technical assistance with the article preparation, Drs Jane Leopold and Wusheng Xiao for sharing their expertise in endothelial biology, and Dr Andriy Samokhin for sharing his expertise in confocal microscopy. The authors thank Dr Andrew Lichtman for the valuable discussion of T cell biology. The authors also thank Dr Zachery Herbert at the Molecular Biology Core Facility, Dana-Farber Cancer Institute, and Dr Grigoriy Losyev at the Brigham and Women's Hospital Flow Cytometry Core Facility.

Sources of Funding

This study was supported in part by the National Institutes of Health grants T32 HL760434 to L.Y.-H.L., HL128802 to W.M.O., HG007690, HL108630, HL119145, HL155096, and HL155107 and American Heart Association grants D700382 and CV-19 to J.L.

Disclosures

Dr Lee designed the study, performed all experiments, analyzed all data, and wrote the article. Dr Oldham provided expertise in metabolomics and performed liquid chromatography mass spectrometry measurements of metabolites. Dr He provided expertise in metabolomics and performed high-performance liquid chromatography measurements of metabolites. Dr Wang analyzed the RNA sequencing study data and provided expert statistical analysis. Mr Mulhern assisted with experiments. Dr Hardy provided critical advice during study design and experiments. Dr Loscalzo designed and supervised the overall study and article preparation. All authors contributed to final approval of the article.

Supplemental Material

Supplemental Methods
Tables S1–S3
Figures S1–S6
References 59–65

REFERENCES

1. Li X, Sun X, Carmeliet P. Hallmarks of endothelial cell metabolism in health and disease. *Cell Metab.* 2019;30:414–433. doi: 10.1016/j.cmet.2019.08.011
2. Krützfeldt A, Spahr R, Mertens S, Siegmund B, Piper HM. Metabolism of exogenous substrates by coronary endothelial cells in culture. *J Mol Cell Cardiol.* 1990;22:1393–1404. doi: 10.1016/0022-2828(90)90984-a
3. Culic O, Gruwel ML, Schrader J. Energy turnover of vascular endothelial cells. *Am J Physiol.* 1997;273(1 pt 1):C205–C213. doi: 10.1152/ajpcell.1997.273.1.C205
4. Yang Q, Xu J, Ma Q, Liu Z, Sudhahar V, Cao Y, Wang L, Zeng X, Zhou Y, Zhang M, et al. PRKAA1/AMPKα1-driven glycolysis in endothelial cells exposed to disturbed flow protects against atherosclerosis. *Nat Commun.* 2018;9:4667. doi: 10.1038/s41467-018-07132-x
5. Cao Y, Zhang X, Wang L, Yang Q, Ma Q, Xu J, Wang J, Kovacs L, Ayon RJ, Liu Z, et al. PFKFB3-mediated endothelial glycolysis promotes pulmonary hypertension. *Proc Natl Acad Sci U S A.* 2019;116:13394–13403. doi: 10.1073/pnas.1821401116
6. De Bock K, Georgiadou M, Schoors S, Kuchnio A, Wong BW, Cantelmo AR, Quaegebeur A, Ghesquière B, Cauwenberghs S, Eelen G, et al. Role of PFKFB3-driven glycolysis in vessel sprouting. *Cell.* 2013;154:651–663. doi: 10.1016/j.cell.2013.06.037
7. Fernandez DM, Rahman AH, Fernandez NF, Chudnovskiy A, Amir ED, Amadori L, Khan NS, Wong CK, Shamailova R, Hill CA, et al. Single-cell immune landscape of human atherosclerotic plaques. *Nat Med.* 2019;25:1576–1588. doi: 10.1038/s41591-019-0590-4
8. Tellides G, Tereb DA, Kirkiles-Smith NC, Kim RW, Wilson JH, Schechner JS, Lorber MI, Pober JS. Interferon-gamma elicits arteriosclerosis in the absence of leukocytes. *Nature.* 2000;403:207–211. doi: 10.1038/35003221
9. Buono C, Come CE, Stavrakis G, Maguire GF, Connelly PW, Lichtman AH. Influence of interferon-gamma on the extent and phenotype of diet-induced atherosclerosis in the LDLR-deficient mouse. *Arterioscler Thromb Vasc Biol.* 2003;23:454–460. doi: 10.1161/01.ATV.0000059419.11002.6E
10. Zohlnhöfer D, Richter T, Neumann F, Nührenberg T, Wessely R, Brandl R, Murr A, Klein CA, Baeuerle PA. Transcriptome analysis reveals a role of interferon-gamma in human neointima formation. *Mol Cell.* 2001;7:1059–1069. doi: 10.1016/s1097-2765(01)00239-8
11. Tellides G, Pober JS. Interferon-gamma axis in graft arteriosclerosis. *Circ Res.* 2007;100:622–632. doi: 10.1161/01.RES.0000258861.72279.29
12. Sakash JB, Byrne GI, Lichtman A, Libby P. Cytokines induce indoleamine 2,3-dioxygenase expression in human atheroma-associated cells: implications for persistent Chlamydophila pneumoniae infection. *Infect Immun.* 2002;70:3959–3961. doi: 10.1128/IAI.70.7.3959-3961.2002
13. Lahdou I, Engler C, Mehrle S, Daniel V, Sadeghi M, Opelz G, Terness P. Role of human corneal endothelial cells in T-cell-mediated alloimmune attack in vitro. *Invest Ophthalmol Vis Sci.* 2014;55:1213–1221. doi: 10.1167/iovs.13-11930
14. Liu R, Merola J, Manes TD, Qin L, Tietjen GT, Lopez-Giraldez F, Broecker V, Fang C, Xie C, Chen PM, et al. Interferon-gamma converts human microvascular pericytes into negative regulators of alloimmunity through induction of indoleamine 2,3-dioxygenase 1. *JCI Insight.* 2018;3:e97881. doi: 10.1172/jci.insight.97881
15. Opitz CA, Litzenburger UM, Sahm F, Ott M, Tritschler I, Trump S, Schumacher T, Jestaedt L, Schrenk D, Weller M, et al. An endogenous tumour-promoting ligand of the human aryl hydrocarbon receptor. *Nature.* 2011;478:197–203. doi: 10.1038/nature10491
16. Hankinson O. The aryl hydrocarbon receptor complex. *Annu Rev Pharmacol Toxicol.* 1995;35:307–340. doi: 10.1146/annurev.pa.35.040195.001515
17. Wang GL, Semenza GL. Purification and characterization of hypoxia-inducible factor 1. *J Biol Chem.* 1995;270:1230–1237. doi: 10.1074/jbc.270.3.1230

18. Wood SM, Gleadle JM, Pugh CW, Hankinson O, Ratcliffe PJ. The role of the aryl hydrocarbon receptor nuclear translocator (ARNT) in hypoxic induction of gene expression. Studies in ARNT-deficient cells. *J Biol Chem.* 1996;271:15117–15123. doi: 10.1074/jbc.271.25.15117
19. Jacob A, Potin S, Saubaméa B, Crete D, Scherrmann JM, Curis E, Peyssonnaux C, Declèves X. Hypoxia interferes with aryl hydrocarbon receptor pathway in hCMEC/D3 human cerebral microvascular endothelial cells. *J Neurochem.* 2015;132:373–383. doi: 10.1111/jnc.12972
20. Ohh M, Park CW, Ivan M, Hoffman MA, Kim TY, Huang LE, Pavletich N, Chau V, Kaelin WG. Ubiquitination of hypoxia-inducible factor requires direct binding to the beta-domain of the von Hippel-Lindau protein. *Nat Cell Biol.* 2000;2:423–427. doi: 10.1038/35017054
21. Xiao W, Wang RS, Handy DE, Loscalzo J. NAD(H) and NADP(H) redox couples and cellular energy metabolism. *Antioxid Redox Signal.* 2018;28:251–272. doi: 10.1089/ars.2017.7216
22. Vita JA, Treasure CB, Nabel EG, McLenachan JM, Fish RD, Yeung AC, Vekshtein VI, Selwyn AP, Ganz P. Coronary vasomotor response to acetylcholine relates to risk factors for coronary artery disease. *Circulation.* 1990;81:491–497. doi: 10.1161/01.cir.81.2.491
23. Loscalzo J. Nitric oxide signaling and atherothrombosis redux: evidence from experiments of nature and implications for therapy. *Circulation.* 2018;137:233–236. doi: 10.1161/CIRCULATIONAHA.117.032901
24. Eroglu E, Saravi SSS, Sorrentino A, Steinhorn B, Michel T. Discordance between eNOS phosphorylation and activation revealed by multispectral imaging and chemogenetic methods. *Proc Natl Acad Sci U S A.* 2019;116:20210–20217. doi: 10.1073/pnas.1910942116
25. Friesel R, Komoriya A, Maciag T. Inhibition of endothelial cell proliferation by gamma-interferon. *J Cell Biol.* 1987;104:689–696. doi: 10.1083/jcb.104.3.689
26. Merchan JR, Kovács K, Railsback JW, Kurtoglu M, Jing Y, Piña Y, Gao N, Murray TG, Lehrman MA, Lampidis TJ. Antiangiogenic activity of 2-deoxy-D-glucose. *PLoS One.* 2010;5:e13699. doi: 10.1371/journal.pone.0013699
27. Wang F, Zhang S, Jeon R, Vuckovic I, Jiang X, Lerman A, Folmes CD, Dzeja PD, Herrmann J. Interferon gamma induces reversible metabolic reprogramming of M1 macrophages to sustain cell viability and pro-inflammatory activity. *EBioMedicine.* 2018;30:303–316. doi: 10.1016/j.ebiom.2018.02.009
28. Shima K, Kaeding N, Ogunsulire IM, Kaufhold I, Klinger M, Rupp J. Interferon-γ interferes with host cell metabolism during intracellular Chlamydia trachomatis infection. *Cytokine.* 2018;112:95–101. doi: 10.1016/j.cyto.2018.05.039
29. Carmeliet P, Dor Y, Herbert JM, Fukumura D, Brusselmans K, Dewerchin M, Neeman M, Bono F, Abramovitch R, Maxwell P, et al. Role of HIF-1alpha in hypoxia-mediated apoptosis, cell proliferation and tumour angiogenesis. *Nature.* 1998;394:485–490. doi: 10.1038/28867
30. Manalo DJ, Rowan A, Lavoie T, Natarajan L, Kelly BD, Ye SQ, Garcia JG, Semenza GL. Transcriptional regulation of vascular endothelial cell responses to hypoxia by HIF-1. *Blood.* 2005;105:659–669. doi: 10.1182/blood-2004-07-2958
31. Tang N, Wang L, Esko J, Giordano FJ, Huang Y, Gerber HP, Ferrara N, Johnson RS. Loss of HIF-1alpha in endothelial cells disrupts a hypoxia-driven VEGF autocrine loop necessary for tumorigenesis. *Cancer Cell.* 2004;6:485–495. doi: 10.1016/j.ccr.2004.09.026
32. Wei H, Bedja D, Koitabashi N, Xing D, Chen J, Fox-Talbot K, Rouf R, Chen S, Steenbergen C, Harmon JW, et al. Endothelial expression of hypoxia-inducible factor 1 protects the murine heart and aorta from pressure overload by suppression of TGF-β signaling. *Proc Natl Acad Sci U S A.* 2012;109:E841–E850. doi: 10.1073/pnas.1202081109
33. Huang Y, Lei L, Liu D, Jovin I, Russell R, Johnson RS, Di Lorenzo A, Giordano FJ. Normal glucose uptake in the brain and heart requires an endothelial cell-specific HIF-1α–dependent function. *Proc Natl Acad Sci U S A.* 2012;109:17478–17483. doi: 10.1073/pnas.1209281109
34. Jiang YZ, Li Y, Wang K, Dai CF, Huang SA, Chen DB, Zheng J. Distinct roles of HIF1A in endothelial adaptations to physiological and ambient oxygen. *Mol Cell Endocrinol.* 2014;391:60–67. doi: 10.1016/j.mce.2014.04.008
35. Akhtar S, Hartmann P, Karshovska E, Rinderknecht FA, Subramanian P, Gremse F, Grommes J, Jacobs M, Kiessling F, Weber C, et al. Endothelial hypoxia-inducible factor-1α promotes atherosclerosis and monocyte recruitment by upregulating microRNA-19a. *Hypertension.* 2015;66:1220–1226. doi: 10.1161/HYPERTENSIONAHA.115.05886
36. Feng S, Bowden N, Fragiadaki M, Souilhol C, Hsiao S, Mahmoud M, Allen S, Pirri D, Ayllon BT, Akhtar S, et al. Mechanical activation of hypoxia-inducible factor 1α drives endothelial dysfunction at atheroprone sites. *Arterioscler Thromb Vasc Biol.* 2017;37:2087–2101. doi: 10.1161/ATVBAHA.117.309249
37. Wu D, Huang RT, Hamanaka RB, Krause M, Oh MJ, Kuo CH, Nigdelioglu R, Meliton AY, Witt L, Dai G, et al. HIF-1α is required for disturbed flow-induced metabolic reprogramming in human and porcine vascular endothelium. *Elife.* 2017;6:e25217. doi: 10.7554/eLife.25217
38. Aune TM, Pogue SL. Inhibition of tumor cell growth by interferon-gamma is mediated by two distinct mechanisms dependent upon oxygen tension: induction of tryptophan degradation and depletion of intracellular nicotinamide adenine dinucleotide. *J Clin Invest.* 1989;84:863–875. doi: 10.1172/JCI114247
39. Grant RS. Indoleamine 2,3-dioxygenase activity increases NAD+ production in IFN-γ-stimulated human primary mononuclear cells. *Int J Tryptophan Res.* 2018;11:1178646917751636. doi: 10.1177/1178646917751636
40. Alano CC, Garnier P, Ying W, Higashi Y, Kauppinen TM, Swanson RA. NAD+ depletion is necessary and sufficient for poly(ADP-ribose) polymerase-1-mediated neuronal death. *J Neurosci.* 2010;30:2967–2978. doi: 10.1523/JNEUROSCI.5552-09.2010
41. Andrabi SA, Umanah GK, Chang C, Stevens DA, Karuppagounder SS, Gagné JP, Poirier GG, Dawson VL, Dawson TM. Poly(ADP-ribose) polymerase-dependent energy depletion occurs through inhibition of glycolysis. *Proc Natl Acad Sci U S A.* 2014;111:10209–10214. doi: 10.1073/pnas.1405158111
42. Fouquerel E, Goellner EM, Yu Z, Gagné JP, Barbi de Moura M, Feinstein T, Wheeler D, Redpath P, Li J, Romero G, et al. ARTD1/PARP1 negatively regulates glycolysis by inhibiting hexokinase 1 independent of NAD+ depletion. *Cell Rep.* 2014;8:1819–1831. doi: 10.1016/j.celrep.2014.08.036
43. Patton JS, Shepard HM, Wilking H, Lewis G, Aggarwal BB, Eessalu TE, Gavin LA, Grunfeld C. Interferons and tumor necrosis factors have similar catabolic effects on 3T3 L1 cells. *Proc Natl Acad Sci U S A.* 1986;83:8313–8317. doi: 10.1073/pnas.83.21.8313
44. Jackson SK, Darmani H, Stark JM, Harwood JL. Interferon-gamma increases macrophage phospholipid polyunsaturation: a possible mechanism of endotoxin sensitivity. *Int J Exp Pathol.* 1992;73:783–791.
45. Xiong J, Kawagishi H, Yan Y, Liu J, Wells QS, Edmunds LR, Fergusson MM, Yu ZX, Rovira II, Brittain EL, et al. A metabolic basis for endothelial-to-mesenchymal transition. *Mol Cell.* 2018;69:689–698.e7. doi: 10.1016/j.molcel.2018.01.010
46. Faulkner A, Lynam E, Purcell R, Jones C, Lopez C, Board M, Wagner KD, Wagner N, Carr C, Wheeler-Jones C. Context-dependent regulation of endothelial cell metabolism: differential effects of the PPARβ/δ agonist GW0742 and VEGF-A. *Sci Rep.* 2020;10:7849. doi: 10.1038/s41598-020-63900-0
47. Schoors S, Bruning U, Missiaen R, Queiroz KC, Borgers G, Elia I, Zecchin A, Cantelmo AR, Christen S, Goveia J, et al. Fatty acid carbon is essential for dNTP synthesis in endothelial cells. *Nature.* 2015;520:192–197. doi: 10.1038/nature14362
48. Patella F, Schug ZT, Persi E, Neilson LJ, Erami Z, Avanzato D, Maione F, Hernandez-Fernaud JR, Mackay G, Zheng L, et al. Proteomics-based metabolic modeling reveals that fatty acid oxidation (FAO) controls endothelial cell (EC) permeability. *Mol Cell Proteomics.* 2015;14:621–634. doi: 10.1074/mcp.M114.045575
49. Kalucka J, Ghesquière B, Fendt SM, Carmeliet P. Analysis of endothelial fatty acid metabolism using tracer metabolomics. *Methods Mol Biol.* 2019;1978:259–268. doi: 10.1007/978-1-4939-9236-2_16
50. Dagher Z, Ruderman N, Tornheim K, Ido Y. Acute regulation of fatty acid oxidation and amp-activated protein kinase in human umbilical vein endothelial cells. *Circ Res.* 2001;88:1276–1282. doi: 10.1161/hh1201.092998
51. Kajihara N, Kukidome D, Sada K, Motoshima H, Furukawa N, Matsumura T, Nishikawa T, Araki E. Low glucose induces mitochondrial reactive oxygen species via fatty acid oxidation in bovine aortic endothelial cells. *J Diabetes Investig.* 2017;8:750–761. doi: 10.1111/jdi.12678
52. Hue L, Taegtmeyer H. The Randle cycle revisited: a new head for an old hat. *Am J Physiol Endocrinol Metab.* 2009;297:E578–E591. doi: 10.1152/ajpendo.00093.2009
53. Berger NA. Poly(ADP-ribose) in the cellular response to DNA damage. *Radiat Res.* 1985;101:4–15.
54. Eleftheriadis T, Pissas G, Sounidaki M, Antoniadi G, Rountas C, Liakopoulos V, Stefanidis I. Correction to: Tryptophan depletion under conditions that imitate insulin resistance enhances fatty acid oxidation and induces endothelial dysfunction through reactive oxygen species-dependent and independent pathways. *Mol Cell Biochem.* 2018;440:221. doi: 10.1007/s11010-018-3277-0
55. Werner-Felmayer G, Werner ER, Fuchs D, Hausen A, Reibnegger G, Schmidt K, Weiss G, Wachter H. Pteridine biosynthesis in human endothelial cells. Impact on nitric oxide-mediated formation of cyclic GMP. *J Biol Chem.* 1993;268:1842–1846.

56. Ng CT, Fong LY, Low YY, Ban J, Hakim MN, Ahmad Z. Nitric oxide participates in IFN-gamma-induced HUVECs hyperpermeability. *Physiol Res.* 2016;65:1053–1058. doi: 10.33549/physiolres.933237
57. Bossaller C, Habib GB, Yamamoto H, Williams C, Wells S, Henry PD. Impaired muscarinic endothelium-dependent relaxation and cyclic guanosine 5'-monophosphate formation in atherosclerotic human coronary artery and rabbit aorta. *J Clin Invest.* 1987;79:170–174. doi: 10.1172/JCI112779
58. Casas JP, Bautista LE, Humphries SE, Hingorani AD. Endothelial nitric oxide synthase genotype and ischemic heart disease: meta-analysis of 26 studies involving 23028 subjects. *Circulation.* 2004;109:1359–1365. doi: 10.1161/01.CIR.0000121357.76910.A3
59. Dobin A, Davis CA, Schlesinger F, Drenkow J, Zaleski C, Jha S, Batut P, Chaisson M, Gingeras TR. STAR: ultrafast universal RNA-seq aligner. *Bioinformatics.* 2013;29:15–21. doi: 10.1093/bioinformatics/bts635
60. Anders S, Pyl PT, Huber W. HTSeq–a Python framework to work with high-throughput sequencing data. *Bioinformatics.* 2015;31:166–169. doi: 10.1093/bioinformatics/btu638
61. Robinson MD, McCarthy DJ, Smyth GK. edgeR: a Bioconductor package for differential expression analysis of digital gene expression data. *Bioinformatics.* 2010;26:139–140. doi: 10.1093/bioinformatics/btp616
62. Samokhin AO, Stephens T, Wertheim BM, Wang RS, Vargas SO, Yung LM, Cao M, Brown M, Arons E, Dieffenbach PB, et al. NEDD9 targets COL3A1 to promote endothelial fibrosis and pulmonary arterial hypertension. *Sci Transl Med.* 2018;10:eaap7294. doi: 10.1126/scitranslmed.aap7294
63. Lazzarino G, Amorini AM, Fazzina G, Vagnozzi R, Signoretti S, Donzelli S, Di Stasio E, Giardina B, Tavazzi B. Single-sample preparation for simultaneous cellular redox and energy state determination. *Anal Biochem.* 2003;322:51–59. doi: 10.1016/j.ab.2003.07.013
64. Leopold JA, Zhang YY, Scribner AW, Stanton RC, Loscalzo J. Glucose-6-phosphate dehydrogenase overexpression decreases endothelial cell oxidant stress and increases bioavailable nitric oxide. *Arterioscler Thromb Vasc Biol.* 2003;23:411–417. doi: 10.1161/01.ATV.0000056744.26901.BA
65. Semenza GL. Hypoxia-inducible factor 1: oxygen homeostasis and disease pathophysiology. *Trends Mol Med.* 2001;7:345–350. doi: 10.1016/s1471-4914(01)02090-1